OPTIMUM DESIGN OF PRESTRESSED HOLLOW CORE SLAB VIA GENETIC ALGORITHM

Karina Barth Ferro[11]
Alessandro Murta Baldi[2]
Élcio Cassimiro Alves[3]

ABSTRACT

The search for more efficient solutions in reinforced concrete buildings is necessary, in view of the industrialization process of the civil construction sector. Within this scenario, the use of hollow core slabs becomes an interesting process, in view of the speed of execution and the possibility of overcoming larger spans. This paper presents a formulation for the design optimization problem of prestressed reinforced concrete hollow core slabs. The procedure was implemented with Matlab, following design guidelines from the ABNT (Brazilian Association of Technical Standards), according to the standards NBR 6118:2023, NBR 14861:2011 and NBR 9062:2017 and using the guide toolbox to build a Graphical interface. The optimization problem was solved using the genetic algorithm feature native to Matlab, considering the minimization of manufacturing cost of the slab as the objective function. Numerical examples show improvements of the final design, with smaller free spans presenting the serviceability limit state (SLS) as the preponderant design restriction, while the design of larger spans is governed by the tensile forces on the upper surface of the slab during prestressing.

Keywords - Hollow Core Slab, Prestress, Genetic Algorithm, Optimization.

PROJETO ÓTIMO DE LAJES ALVEOLARES PROTENDIDAS VIA ALGORITMO GENÉTICO

RESUMO

A busca por soluções mais eficientes em edifícios de concreto armado é necessária, em vista do processo de industrialização do setor de construção civil. Nesse cenário, o uso de lajes alveolares torna-se um processo interessante, em vista da velocidade de execução e da possibilidade de vencer vãos maiores. Este artigo apresenta uma formulação para o problema de otimização do projeto de lajes alveolares de concreto protendido. O procedimento foi implementado no Matlab, seguindo as diretrizes de projeto de acordo com as normas brasileiras e usando a toolbox do guia para construir uma interface gráfica. O problema de otimização foi resolvido usando o algoritmo genético nativo do Matlab, considerando a minimização do custo de fabricação da laje como função objetivo. Exemplos numéricos foram analisados de forma a validar a otimização e os resultados demonstraram promissores no projeto final, com vãos livres menores apresentando o estado limite de serviço como a restrição de projeto preponderante, enquanto para os vãos maiores o estado governante foi as forças de tração na superfície superior da laje durante a protensão.

Palavras-chave - Laje Alveolar, Protensão, Algoritmo Genético, Otimização

[1] Departamento Engenharia Civil – Universidade Federal do Espírito Santo. E-mail: karina.ferro@edu.ufes.br
[2] Departamento de Computação – Universidade Federal do Espírito Santo. E-mail: alessandro.baldi@edu.ufes.br
[3] Departamento Engenharia Civil – Universidade Federal do Espírito Santo. E-mail: elcio.alves@ufes.br

INTRODUCTION

The industrialization and economic development of the world were the main factors leading to the industrialization of civil construction processes. The demand for faster building assembly and slenderer structures with ever-increasing span lengths stimulated the use of prefabricated concrete elements, and subsequently, the installation of an industry for prefabricated structures.

Prefabricated concrete structures provided speed, quality, and reduction of labor-related costs in civil construction, and, along with prestressing techniques, allowed the construction of structures featuring more headroom and larger free spans.

After consolidated in the United States and Europe, industries of prefabricated concrete structures began being installed in Brazil. Starting in the '1970s after the development of extrusion machines and molds for concrete elements, a popularization of alveolar panels was observed, usually implemented in buildings as floor slabs or enclosure elements.

Recent studies such as those presented by Motlagh and Rahai (2022) and Maghsoudi and Maghsoudi (2019) demonstrate the importance of structures via numerical or experimental analysis of the effects of prestressing on reinforced concrete elements in the short and long term.

Cheng et al. (2021) presents a study of Flexural performance test of a prestressed concrete beam with plastic bellows and Low et al. (2019) analyzed in the experimental and numerical study the interface slip of post-tensioned concrete beams with stage construction.

According to NBR 9062:2017, prefabricated elements are industrially produced by companies focused on this activity, using rigorous technological controls, specialized labor and machinery capable of providing quality and efficiency to the fabrication process. These elements are produced in factories outside of the building site in which they will be installed, eliminating the need for on-site installations to perform technological controls.

Since they are prefabricated concrete elements featuring prestressed tendons, hollow core slabs present various benefits, which include reduction of weight due to the empty spaces resulting from the extrusion of alveoli, capacity of covering longer spans using slabs with reduced thickness and rigorous technological control, thus ensuring the quality and efficiency of structural elements, along with reducing labor costs attributed to construction. Floor systems featuring hollow core slabs present faster production and assembly since there is no need for shuttering and on-site formwork. These elements may be used in a variety of structural systems such as prefabricated concrete, cast-in-place concrete, structural masonry and steel-concrete composite systems.

The application of optimization techniques to the design of structural elements has increased in recent decades, as observed in the papers published by Senouci and Al-Ansari (2009), Erdal, Dogan and Saka (2011), Kripka, Medeiros and Lemonge (2015), Santoro and Kripka (2020), Tormen et al. (2020), Luévanos-Rojas et al. (2020), among others.

However, as stated by Lippiatt (2007), Paya-Saforteza et al. (2009), Camp and Huq (2013), Park et al. (2014), Yepes, Martí and García-Segura (2015), Kaveh and Ardalani (2016), Santoro and Kripka (2020) and Tormen et al. (2020), Kaveh et al.(2020), Kaveh et al.(2022) optimization procedures focused solely on financial costs may not be sufficient to determine the optimal design of a structure. Environmental impact studies, that account for the life-cycle of materials and their effects on the natural environment became an important factor that should also be considered.

Among the bioinspired methods usually implemented to solve optimization problems, Genetic Algorithms (GA) are one of the most prominent. This method is based on the principles of Darwinian natural selection and its formulation was first introduced by John Holland during the 60's. GA is based on selecting from an initial population with or without restrictions, parent individuals to form a new

generation composed of increasingly apt individuals, i.e., the offspring. After several iterations, individuals corresponding to improved solutions are selected, and the final group is regarded as the optimal solution to the problem.

Cho et al. (2001) performed an optimization study using GA to evaluate the life cycle of bridges featuring orthotropic steel decks, which consist of ribbed steel sheets reinforced transversely, longitudinally, or in both directions. Since this was a life-cycle analysis, the study considers initial and maintenance costs of the structure, with adjustments in strength, deflection and fatigue of the structure. The study concludes that the optimization analyses lead to a more rational, economical and safer design when compared to conventional methods.

Kuan-Chen Fu et al. (2005) used GA to determine the optimal design of welded steel girder bridges, with the chief objective of minimizing the weight, and consequently the cost of the structure. The study includes beams of single and continuous spans with different lengths, and results show that GA yields satisfactory results, highlighting the similarity between GA designs and real-world structures when discrete variables are adopted.

Kripakaran et al. (2011) developed a decision-making support system based on GA for the structural optimization of rigid steel frames with variations in connection type. The authors also highlight the advantages of using GA with discrete variables. This characteristic is explored by the program subsequently presented herein.

Kociecki and Adeli (2015) used GA as part of an optimization program for steel structures and Prendes-Gero et al. (2018), who applied the same method to optimize steel frames basing formulations on different design standards, observed improvements of approximately 10% in comparison to non-optimized designs. Both studies also point to the possibility of using discrete variables when applying GA as an important tool for reaching satisfactory results.

Akbari and Ayubirad (2017) studied the optimum design of steel structures using Gradient Gased and Genetic Algorithm. The authors compared the use of Genetic Algoritm with do Sequential Quadratic Programming for different steel frames structures.

Malveiro et al. (2018) implemented GA on a study of bridges and viaducts, featuring numerical models validated by experimental data. The algorithm was used to calibrate parameters, calculating optimal values for the most significant physical properties with the objective of increasing the correlation between numerical and experimental results.

Yildirim and Akcay (2019) proposed a model for reducing the time and cost of the development of projects using GA in combination with the Fuzzy logic.

Aydin (2022) did a study aimed at optimizing the costs of prestressed steel trusses using cables positioned below the lower flange and molded with desviators. The optimization variables defined were the sections of the elements and layout of the truss, cable profile, dimension of the desviators. The optimization algorithm used was Jaya. Through the results it was observed that the pretension provided a savings in the costs of the steel truss project.

Vahidi et al. (2019) uses genetic algorithm (GA), particle swarm (PSO) and artificial bee colony (ABC) algorithms to investigate the damage detection problems. A hybrid multistage optimization method is presented merging advantages of PSO and ABC methods in finding damage location and extent. The efficiency of the methods has been examined using two simulated numerical examples, a laboratory dynamic test and a high-rise building field ambient vibration test result. The implemented evolutionary updating methods show successful results in accuracy and speed considering the incomplete and noisy experimental measured data.

Guimaraes et al. (2022) present a study of composite column filled with concrete where GA was used to find the best solution. Authors analyses the CO_{KN} emission of the columns and concluded that the best solution was to circular profile.

Netto et al. (2023), performed the analysis and comparison of the optimized design of prestressed steel beam using doubly symmetric and monosymmetric profiles. The solutions with monosymmetric profile were better than with doubly symmetric profiles.

Fiorotti et al. (2023) presents a study of prestressed steel beams where the optimization problem solution was obtained by GA.

Although several works are found in the literature with the application of the genetic algorithm and several works involving the effect of prestressing in concrete and steel structures, no work has yet been found on the optimization of hollow core slabs using metaheuristic algorithms. The objective of this paper is to present a formulation for optimizing the design of prestressed concrete hollow core slabs. The number of prestressing cables, the height of the concrete layer and the final geometry of the slab were considered as design variables. A computer program was developed with MATLAB© and the solution was obtained using the native genetic algorithm toolbox to solve the optimization problem.

OPTIMIZATION PROBLEM FORMULATION

For the problem at hand, the optimized design of hollow core slabs uses discrete variables, extracted from a product catalogue of this type of structural element provided by the company Cassol Pré-Fabricados, along with a catalogue containing prestressing tendon dimensions, provided by Belgo Bekaert Arames. The objective function must converge to a minimum value to reduce the cost of the materials used for producing the slabs, that is, volume of concrete and weight of prestressing tendons, while also minimizing the thickness of the upper portion of the slab cross-section, resulting in dimensions that meet the restrictions imposed by a pertinent design standard.

Objective Function

The objective function must minimize the costs of steel and concrete attributed to producing the hollow core slab. Equation (1) represents the formulation for obtaining the final cost, considering the concrete and the prestressing tendon.

$$f(x) = (Ct_c \, A_{simple \, section} + Ct_p n_{tendon} \, \mu_p) l_{span} \tag{1}$$

Where: Ct_c is the price per m³ of concrete; A simple section is the area of concrete of the hollow core slab cross-section; Ct_p is the price of the tendon per kg; ntendon is the number of tendons; µp is the linear mass of one tendon, in kg/m; lspan is the length of the slab, in m. The cost per unit of concrete and prestressing tendon are presented in Table 1.

Table 1 – Cost of materials.

7 strand tendon - CP190 RB		Concrete	
Nominal diameter (mm)	Cost (R$/kg)	f_{ck} (MPa)	Cost (R$/m³)
9.5	9.31	20	290.00
12.7	8.84	25	307.42
15.2	8.84	30	317.77

15.7	9.46	35	329.15
7 strand tendon - CP210 RB		40	341.57
12.7	9.98	45	384.01
15.2	9.98	50	455.43
Source	**Local supplier**		**Sinapi (2022)**

Constraint Functions

The constraints of the optimization problem are based on the design criteria from the standards NBR 6118:2023, NBR 14861:2011 and NBR 9062:2017. These constraints were imposed to ensure that the design of the hollow core slab meet the limits imposed by Ultimate (ULS) and Serviceability (SLS) limit states. The constraints are presented in Eq. (2) to Eq. (21):

$$C(1): 4 \times 0{,}272 \times KMD - 0{,}68^2 \leq 0 \tag{2}$$

$$C(2): h_{effective} - h_{layer}/KX \leq 0 \tag{3}$$

$$C(3): 2 - n_{tendon} \leq 0 \tag{4}$$

$$C(4): n_{tendon} - (n_{alv} + 1) \leq 0 \tag{5}$$

$$C(5): \frac{f_{ctm,j}}{1{,}2} - \sigma_{s,ELU} \leq 0 \tag{6}$$

$$C(6): \sigma_{i,ELU} - 0{,}85 \times \frac{f_{cj}}{1{,}3} \leq 0 \tag{7}$$

$$C(7): \sigma_{s,ELS-D} \geq 0 \tag{8}$$

$$C(8): \sigma_{s,ELS-D} - 0{,}85 \times \frac{f_{ck}}{1{,}4} \leq 0 \tag{9}$$

$$C(9): \sigma_{s,ELS-F} - 0{,}7 \times f_{ctm} > 0 \tag{10}$$

$$C(10): \sigma_{s,ELS-F} - 0{,}85 \times \frac{f_{ck}}{1{,}4} \leq 0 \tag{11}$$

$$C(11): \sigma_{i,ELS-D} \geq 0 \tag{12}$$

$$C(12): \sigma_{i,ELS-D} - 0{,}85 \times \frac{f_{ck}}{1{,}4} \leq 0 \tag{13}$$

$$C(13): \sigma_{i,ELS-F} - 0{,}7 \times f_{ctm} > 0 \tag{14}$$

$$C(14): \sigma_{i,ELS-F} - 0{,}85 \times \frac{f_{ck}}{1{,}4} \leq 0 \tag{15}$$

$$C(15): a_{total,0} - \frac{l_{span}}{350} \leq 0 \tag{16}$$

$$C(16): a_{total,\infty} - \frac{l_{span}}{250} \leq 0 \tag{17}$$

$$C(17): V_{Sd,simple} - V_{Rd1,simple} \leq 0 \tag{18}$$

$$C(18): V_{Sd,simple} - V_{Rd2,simple} \leq 0 \tag{19}$$

$$C(19): V_{Sd,composite} - V_{Rd1,composite} \leq 0 \tag{(}$$

$$C(20): V_{Sd,composite} - V_{Rd2,composite} \leq 0 \quad (21)$$

Where: *KMD* is admensional factor, *KX* is neutral line position, $h_{effective}$ is the effective depth of the cross-section, ; h_{layer} is the height of the concrete layer; n_{tenodn} is the number of tendons; n_{alv} is the number of alveoli of the slab; in %; $\sigma_{s,ELU}$ is the stress on the upper surface of the slab, for ULS and prestressing age t=0; $\sigma_{i,ELU}$ is the stress on the bottom surface of the slab for ULS and t=0; f_{ctm} is the average tensile strength of concrete; f_{cj} is the compressive strength of concrete at the age of prestressing; σ_{ELS-D} is the stress on superior and inferior surfaces of the slab for SLS-Decompression; σ_{ELS-F} is the stress on superior and inferior surfaces of the slab, for SLS-Crack opening; $a_{total,0}$ is the deflection, considering prestressing force and the weight of the slab; $a_{total,\infty}$ is the total deflection, considering long-term loading; l_{span} is the length of the slab, in m; $V_{Sd,simple}$ is the design shear force acting on the critical cross-section, considering the gross section of the hollow core slab; $V_{Sd,composite}$ is the design shear force acting on the critical cross-section of the slab, considering the concrete layer on the slab; V_{Rd1} is the design resistance to shear force of the slab and V_{Rd2} is the design resistance to shear force of the compressed diagonals of concrete.

Constraint C(1) relates *KMD* and *KX*, and obtain the real value of *KX*. C(2) verifies that the neutral axis crosses the upper layer of concrete; Constraint C(3) determines the minimum number of tendons on the cross-section. According to NBR 14861:2011, the maximum allowable distance between tendons is 400 millimeters or twice the height of the hollow core slab, thus, a minimum of two tendons is required for slabs with a width of 125cm; C(4) establishes the maximum number of tendons for each section of the hollow core slab, with one tendon for each value of web thickness; C(5) and C(6) determine the allowable limits of tension and compression for ULS design at the time of prestressing, on the top and bottom surfaces of the slab, respectively; C(7) and C(8) define the allowable stress on the upper surface of the slab according to SLS-Decompression criteria. Similarly, C(9) and C(10) define the limits for SLS-Crack opening; C(11) and C(12) establish stress limits at the bottom surface of the slab for SLS-Decompression. Analogously, C(13) and C(14) apply constraints related to SLS-Crack opening.

C(15) and C(16), verify deformation limits, considering the combined incidence of prestressing force and structural weight, and long-term loading, respectively; C(17) and C(18), verify the applied shear force and the resistance to shear force of the gross cross-section, necessary to ensure the adequate resistance of the structure during production and assembly. Similarly, C(19) and C(20), verify the applied shear force and the resistance to shear force for the composite section, that is, with strength contributions from the concrete layer during service.

RESULTS AND DISCUSSIONS

Results obtained with the program Alveolaje 2.0, developed for this research, were compared with analyses presented in other research papers. A graphical analysis is also presented subsequently.

3.1. Validation Example

To validate the program Alveolaje 2.0, it is necessary to verify results of the structural analysis. To demonstrate the application and advantages of the computational tool developed, results were compared with the program developed by Ferro and Alves (2019). The validation example is also studied by Camillo (2012). However, this paper does not consider the type of aggregate used for mixing the

concrete. As prescribed by the latest update of NBR 6118:2023, it is necessary to choose an aggregate type. The input data used for this example is given in Table 2.

Table 2 – Input data for the validation example.

INPUT DATA	
Class of environmental aggressiveness	CAA II
Cement type	CP V
Slump	0
$f_{ck\ slab}$	50 MPa
f_{cj}	28 MPa
Prestressing age	20 h
$f_{ck\ layer}$	25 MPa
Aggregate type	BASALT
Free span of the slab	9 m
Serviceability live-load	4.25 kN/m²
Load due to flooring	0.25 kN/m²
Slab height	20 cm
Layer thickness	5 cm

For the given initial parameters used on the design of the hollow core slab, the optimum values of slab height and layer thickness are identical to those presented by Camillo (2012), the former equal to 20 cm, and the latter, 5 cm. Figure 1 presents the cross-section of the slab adopted for the present research. The shape of the cross-section was provided by a local manufacturer.
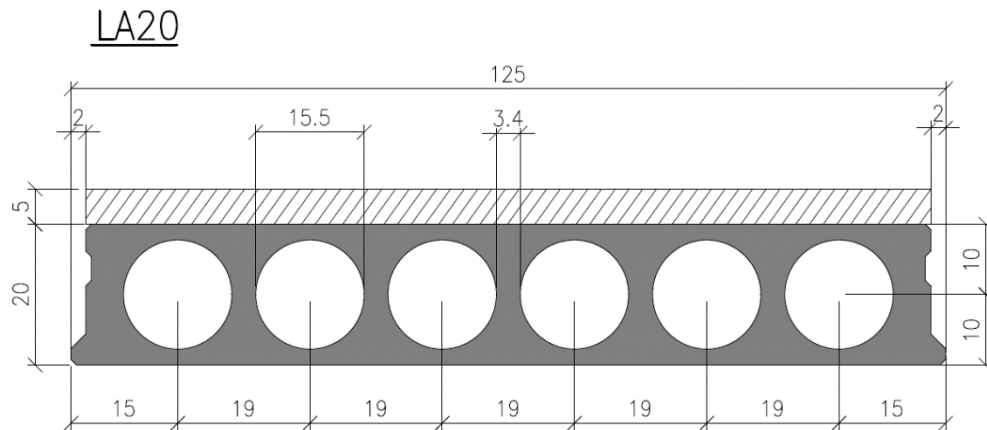
Fig. 1 - Cross-section of the hollow core slab h=20cm and concrete topping h=5cm (dimensions in cm).

Table 3 shows the results obtained for the simple section, considering only the concrete slab, and for the composite section, which includes the slab and a 5cm concrete layer. The table presents values for cross-sectional area, distance between the center of gravity and the upper surface, (Ys), Moment of inertia, superior and inferior elastic section moduli Ws and Wi, respectively, and tendon eccentricity (e). For comparison, results obtained by Ferro and Alves (2019) are also presented.

As expected, the geometric properties have different values. Ferro and Alves (2019) present results

for a rectangular cross-section and centralized openings, the program developed for this research, on the other hand, considers a cross-section featuring shear keyways. As such, the cross-sectional area of the optimized design is smaller in comparison with results presented by Ferro and Alves (2019).

Table 3 presents the initial losses of prestressing force. Values obtained for stresses due to anchorage slip, tendon relaxation and elastic shortening of concrete are given, along with other relevant design variables and the total cost of the slab. All of these values are compared with results obtained by Ferro and Alves (2019).

The optimized cross-section and results obtained for each relevant design parameter are presented by the software GUI shown in Figure 2.

Table 3 – Geometric properties of the simple and composite cross-sections.

	Simple Section - LA20		Composite Section - LA20 and $h_{layer}=5$	
	Authors (2020)	Ferro and Alves (2019)	Authors (2020)	Ferro and Alves (2019)
Area (cm²)	1289.77	1439.71	1914.77	2064.71
Ys (cm)	10.11	10.00	10.99	11.22
Inertia (cm⁴)	64257.71	68423.04	132506.03	147850.12
Ws (cm³)	6355.67	6842.3	12052.39	13181.86
Wi (cm³)	6497.44	6842.3	9460.77	10726.35
e (cm)	7.39	7.5	11.51	11.28
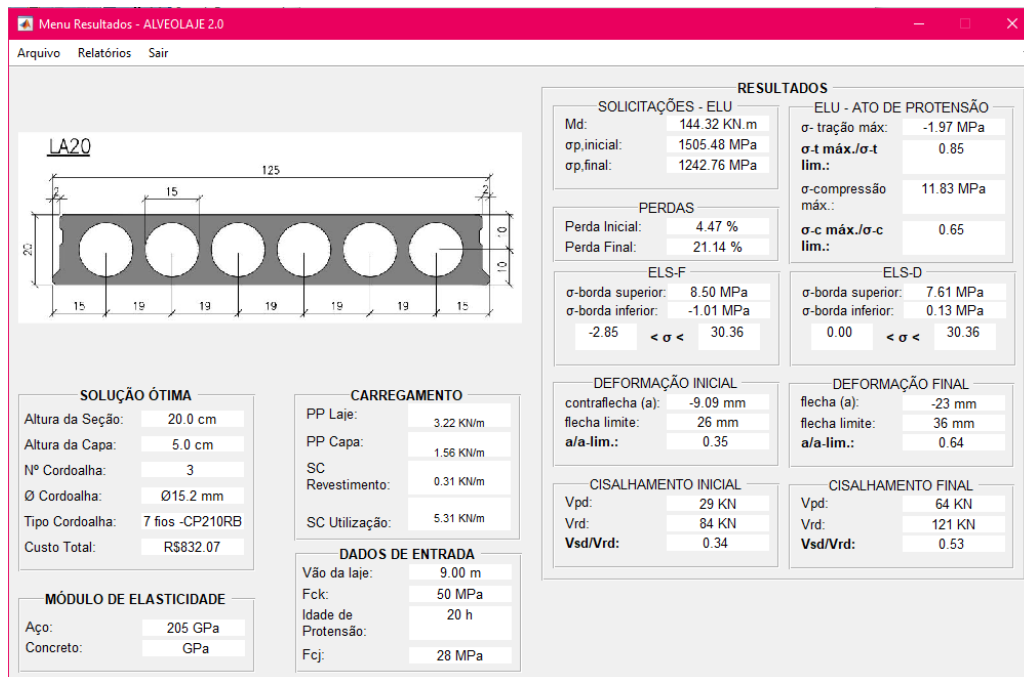
Fig. 2 – Software Validation results.

Values of anchorage slip stress are identical in both studies since they depend on the length of the prestressing track, taken here as 150 meters. The immediate strain on concrete presents a value lower than that presented by Ferro and Alves (2019), because of the different elasticity moduli values used for concrete. The initial loss in prestressing force obtained with the optimization procedure is 19.7% smaller than the values obtained by Ferro and Alves (2019).

Stresses attributed to concrete creep depend directly on the geometric properties of the cross-section. As such, the values obtained were expected. The total loss of prestressing force is 13.4% lower if compared with Ferro and Alves (2019). Table 4 presents results for ULS design at $t=t_\infty$. The optimization procedure presented herein yielded a steel reinforcement area 8.7% smaller than the one indicated by Ferro and Alves (2019).

Maximum values observed for tensile and compressive stresses are within standardized limits for ULS design when $t=t_0$. The length of force transference obtained with the optimization procedure is of 24.04 cm, along which the maximum stresses on the section occur.

Stresses obtained for SLS criteria are also within the limits prescribed by the standard, that is, $0\ MPa < \sigma_{ELS-D} < 30.4\ MPa$, for SLS-Decompression, and $-2.9\ MPa < \sigma_{ELS-F} < 30.4\ MPa$, for SLS- Crack opening.

The optimized deflection shows larger values as a result of a smaller moment of inertia of the cross-section, nonetheless, values remain within standardized limits. It is observed that the shear force acting on the element is 7% smaller for the simple section and 3.3% smaller for the composite section. This reduction in internal force is a direct result of lower dead loads attributed to the weight of the structure. For this example, the optimized design presents a final cost of R$ 832.07, featuring the same slab height as the original design, with 3 CP210RB tendons with a diameter of 15.2 mm. On the other hand, Ferro and Alves (2019) present a final cost of R$922.68 and 9 CP190RB tendons with a diameter of 9.5 mm. As such, results show that the software developed for the present research meets all requirements pertaining to the structural analysis. Furthermore, the reductions observed for prestressing steel area and the number of tendons generated an economy of 9.82% in the cost of materials.

Table 4 – Results from the validation example

	Authors	Ferro and Alves (2019)
Anchorage slip (MPa)	8,2	8.2
Prestressing steel relaxation (MPa)	16.78	15.17
Immediate strain on concrete (MPa)	45.52	58.87
Initial loss	0.0447	0.0577
Concrete creep (MPa)	30.09	46.17
Concrete shrinkage (MPa)	-115.26	-114.82
Prestressing steel relaxation (MPa)	117.37	104.75
Final prestressing loss	0.2114	0.244
Design stress (MPa)	1666.4	1506
Area of steel (cm²)	4.192	4.591
Final prestressing loss	0.2114	0.244
$\sigma_{s.ELS-D}$ (MPa)	7.6	7.3

	Authors	Ferro and Alves (2019)
$\sigma_{i.ELS-D}$ (MPa)	0.1	0
$\sigma_{s.ELS-F}$ (MPa)	8.5	8.1
$\sigma_{i.ELS-F}$ (MPa)	-1.0	-1.2
Initial deflection (mm)	9.09	8.98
Maximum induced camber (mm)	25.71	25.71
Total deflection (mm)	23.22	18.82
Maximum deflection (mm)	36	36
Simple Section		
V_{Rd1} (kN)	83.63	89.37
V_{Rd2} (kN)	282.24	308.7
V_{Sd} (kN)	28.71	30.9
Composite Section		
V_{Rd1} (kN)	120.55	128.84
V_{Rd2} (kN)	578.57	632.81
V_{Sd} (kN)	64,14	66,34
h_{slab}(cm)	20	20
h_{layer}(cm)	5	5
	Authors	**Ferro and Alves (2019)**
n_{tendon}	3	9
d_{tendon}(mm)	15,2	9,5
Steel$_{tendon}$	CP210RB	CP190RB
Final Cost R$	**832,07**	**922,68**

3.2. Parametric Analysis

To evaluate the behavior of different optimized designs of prestressed hollow core slabs as a function of span, the cost per slab unit was analyzed, considering the input data given in Table 5, with variations of span length. The data used for this analysis are identical to those implemented on the validation example.

Table 5 – Input data for the graphical analysis of results.

| INPUT DATA	
Class of environmental aggressiveness	CAA II
Cement type	CP V
Slump	0
$f_{ck\ slab}$	50 MPa
f_{cj}	28 MPa
Prestressing age	20 h
$f_{ck\ layer}$	25 MPa
Aggregate type	BASALT
Free span of the slab	varies

Serviceability live-load	4,25 KN/m²
Load due to flooring	0,25 KN/m²

Table 6 shows detailed results for multiple slab lengths under analysis, obtained for each iteration of the program using the input data from Table 5.

Table 6 – Optimized results for spans between 5 and 9 meters.

Span (m)	Section height (cm)	Layer thickness (cm)	Ø Tendon (mm)	Type	Nº of Tendons	Total Cost
5.00	15	8	12.7	CP 190 RB	2	R$308.64
5.50	15	5	12.7	CP 210 RB	2	R$349.44
6.00	15	5	15.2	CP 190 RB	2	R$405.80
6.50	15	5	15.2	CP 210 RB	2	R$456.31
7.00	15	6	12.7	CP 190 RB	4	R$530.12
7.50	15	5	15.2	CP 190 RB	3	R$581.91
8.00	20	6	12.7	CP 190 RB	4	R$693.96
8.50	20	5	15.2	CP 190 RB	3	R$753.11
9.00	20	5	15.2	CP 210 RB	3	R$832.07
9.50	20	6	12,7	CP 210 RB	5	R$933,48

Figure 3 presents the graph for the evolution of final cost as a function of free span for manufacturing one unit of hollow core slab. The graph shows a linear behavior of the results obtained, indicating coherence. It is worth noting that, for the present analysis, costs attributed to the layer of concrete are not included, since this is a different design variable. For hollow core slabs featuring a width of 1250 mm, the final cost of each slab for spans between 5 and 9 meters range from R$300 to R$850.
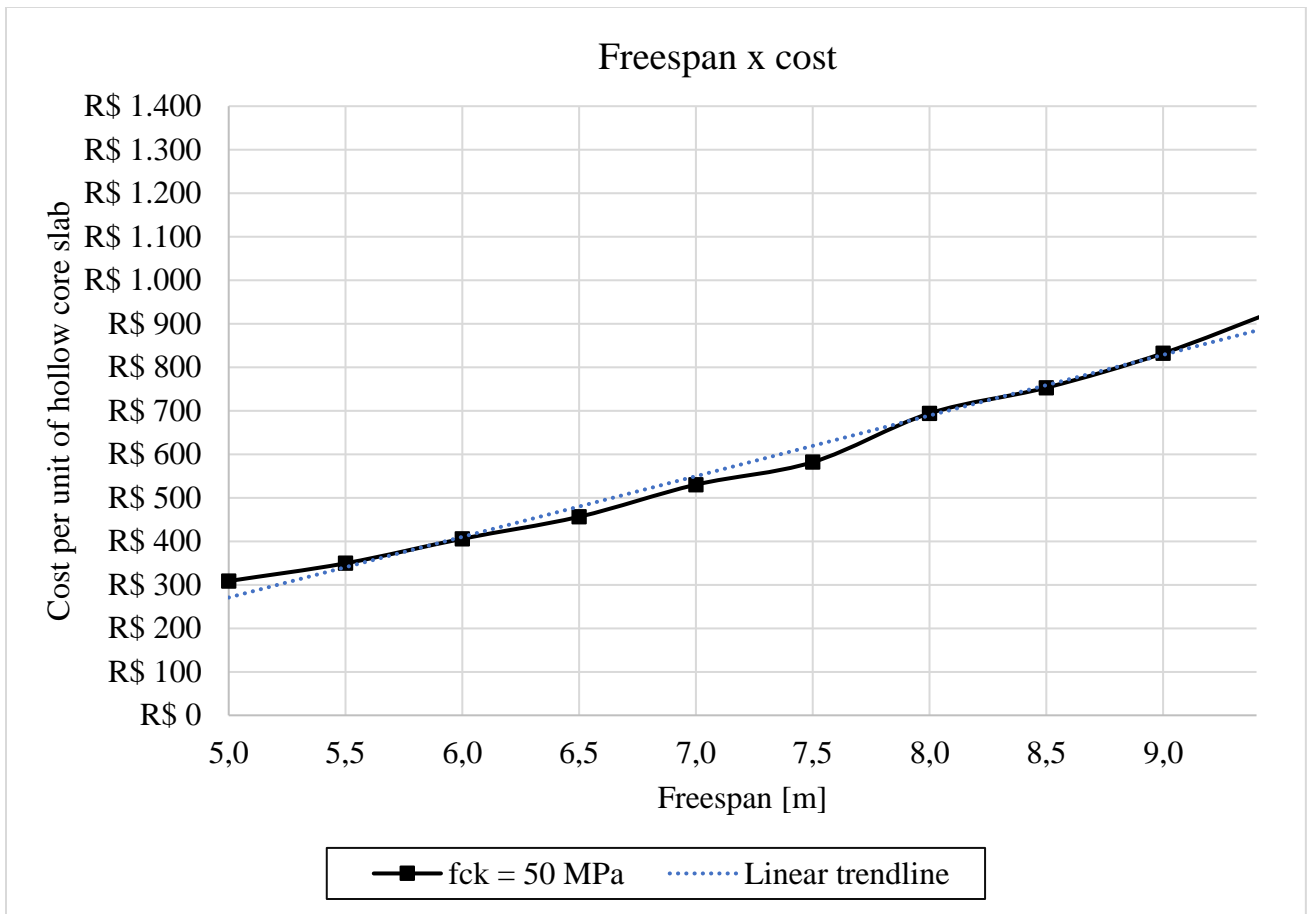
Fig. 3 - Evolution of Freespan x cost for one unit of hollow core slab.

The results presented in Table 6 show that, in order for the designs to meet ULS and SLS criteria, while also reducing the cost per unit of the hollow core slab, the number of tendons must be reduced, and present a diameter of 12.7 mm and 15.2 mm. The number of tendons varies between 2 and 5, with cross-section heights of 15 cm and 20 cm. The final solution is illustrated in the Table 7.

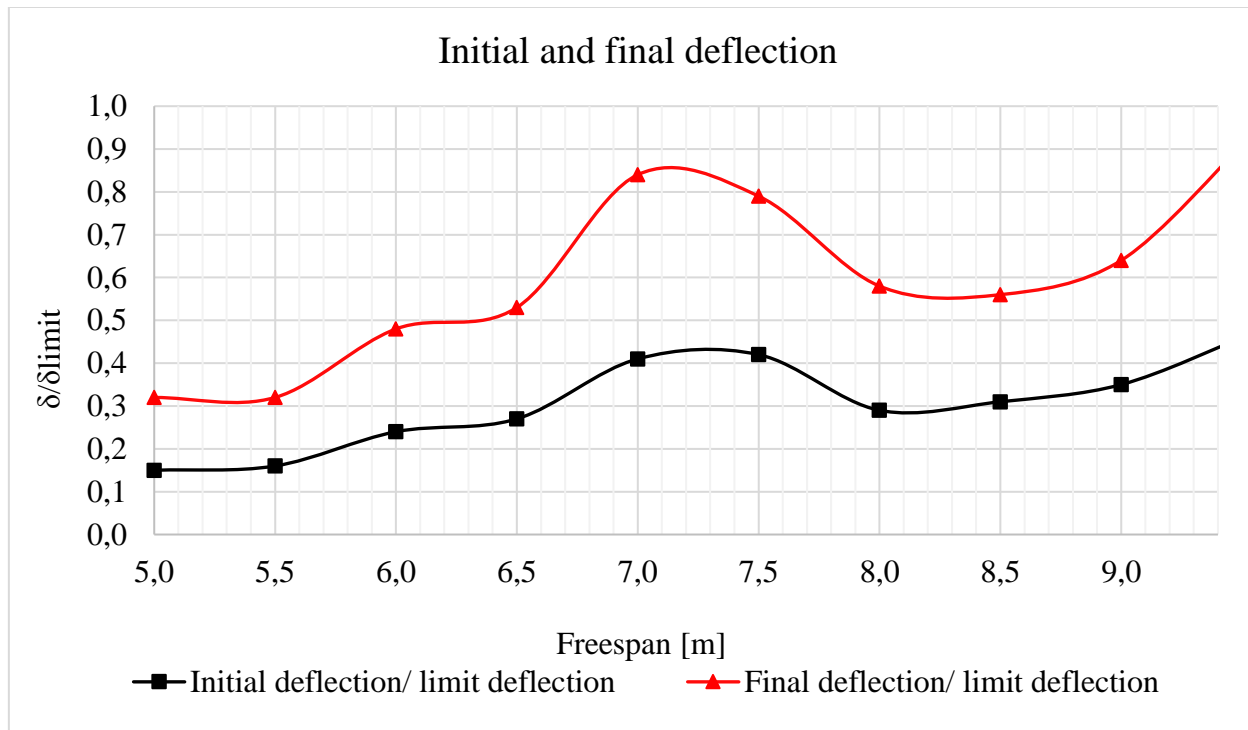**Table 7 –** Final Solution Details.

Span(m)	Geometric Details
5.0, 5.5, 6.0, 6.5	
7.0	

7.5	
8.0	
8.5, 9.0	
9.5	
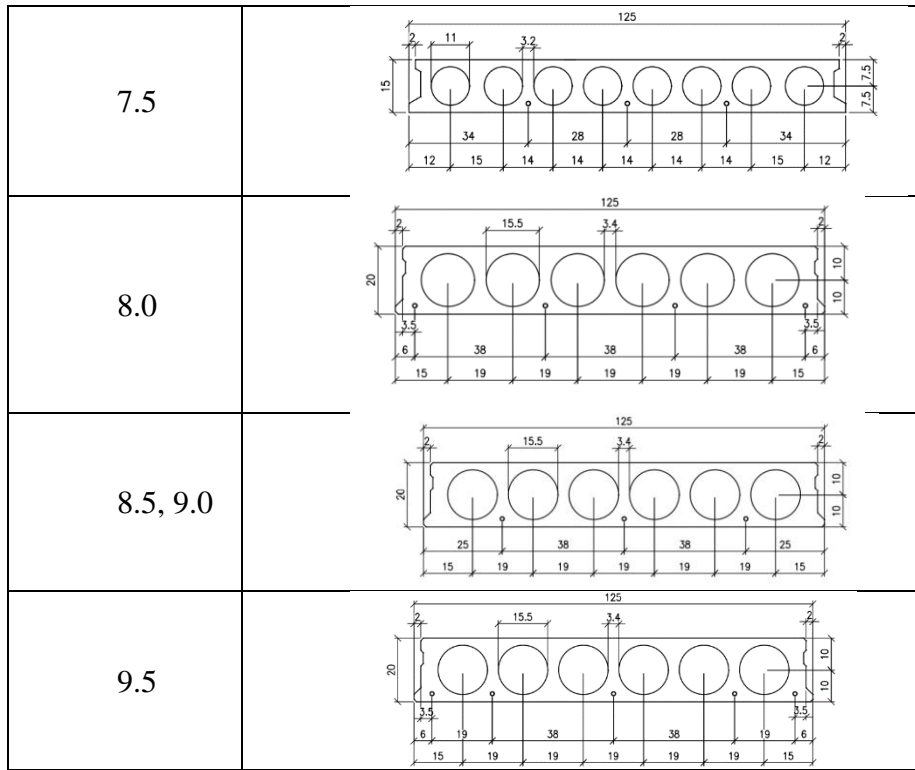
In addition to analyzing the financial cost, the evolution of stresses on the concrete at the time of prestressing is also analyzed, along with initial and final deflection analyses in Figure 4.
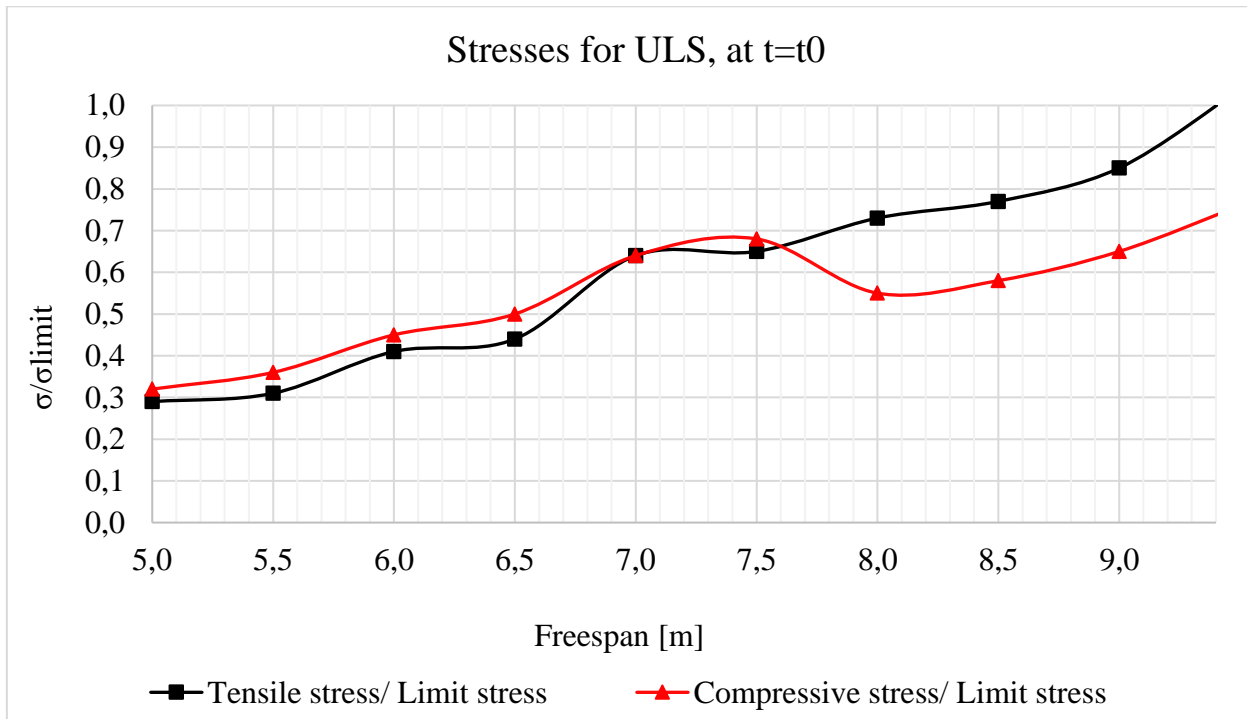
(a)

(b)
Fig. 4 - (a)Graph of stresses for ULS at the time of tendon prestressing; (b) – Maximum deflection.

Figure 4 (a) presents the evolution of tensile and compressive stresses on concrete during prestressing, for a span interval between 5 and 9 meters. The graph shows a linear behavior of the curve for spans ranging from 5 to 7.5 m, however, larger spans indicate a decrease in compressive stress values and an increase of tensile stress on the structure, reaching the maximum values established by NBR 6118:2023 and NBR 14681:2011, for a span of 9.4 meters. From this point on, excessive tension is observed at the time of prestressing, resulting in crack openings, consequently rendering the structural element obsolete. This problem may be solved by introducing additional rebar on the upper flange of the hollow core slab, but there may be constructive limitations if this solution is adopted.

The evolution of initial and final deflections as a function of span length was also performed (Figure 4(b)). The graph from Figure 4, shows that spans between 5 and 7 meters exhibit a tendency to approach standardized limits, resulting in better utilization of allowable values. However, spans ranging from 7 to 9 meters, present small structural deflection.

A combined assessment of the graphs for ULS stresses and deflections, Figure 4(a) and Figure 4(b), respectively, show that deflections of the structure govern the design for spans between 5 and 7 meters. Alternatively, spans between 7 and 9 meters present tensions in the prestressing cables close to the permissible limits, resulting in compression forces on the upper surface of the concrete close to the permissible limit of the design concrete strength.

For slabs with lengths superior to 9 meters, the design is only possible if additional rebar is introduced at the upper surface of the hollow core slab. The design must be performed in a manner analogous to the procedure proposed in this research and consider standardized criteria.

CONCLUSIONS

The results obtained from the design optimization of hollow core slabs were satisfactory, presenting low costs attributed to building materials. For the example analyzed, a cost reduction of 9.82% was observed, which represents a significant saving when evaluating the final production cost of the hollow core slab. As such, the developed program shows relevant applicability.

The parametric analysis provided coherent results for the optimization problem implemented, since smaller slab lengths feature a minimal number of prestressing tendons and, as the length increased, the number of tendons used for prestressing also increased, consequently leading to higher financial costs for producing the slabs. The assessment of cost as a function of span length for the hollow core slabs showed an approximately linear relationship between these variables. The analyses of shorter spans indicated the SLS as the preponderant design criteria, since deflection values were close to the limits established by design standards. For longer spans, it is noted that stresses were the governing restriction, given the increase in the number of prestressing tendons and consequently, the increase of tensile stresses on the upper surface of the slab.

ACKNOWLEDGEMENTS

REFERENCES

ASSOCIAÇÃO BRASILEIRA DE NORMAS TÉCNICAS. NBR 14861: Laje Pré Fabricada – Painel Alveolar de concrete protendido - Requisitos and procedimentos. Rio de Janeiro, 2011.

ASSOCIAÇÃO BRASILEIRA DE NORMAS TÉCNICAS. NBR 6118: Projeto de Estruturas de Concreto. Rio de Janeiro, 2023.

ASSOCIAÇÃO BRASILEIRA DE NORMAS TÉCNICAS. NBR 9062: Projeto e execução de estruturas pré fabricadas. Rio de Janeiro, 2017.

AKBARI J, AYUBIRAD, M.S. (2017). Seismic Optimum Design of Steel Structures Using Gradient-Based and Genetic Algorithm Methods International Journal of Civil Engineering, vol. 15, 135-148.

AYDIN, Z.(2022) Size layout and tendon profile optimization of prestressed steel trusses using Jaya algorithm. Structures. p. 284-294.

CAMILO C.A (2012), Panel Continuity of Hollow core slabs in Building. Master's Thesis in Civil Eingineering – Federal University of São Carlos, São Carlos,. (In Portuguese)

CAMP C.V, HUQ F. CO_2 and cost optimization of reinforced concrete frames using a big bang-big crunch algorithm. Engineering Structures, v. 48, p. 363-372, 2013.

CHO, H., MIN, D., LEE, K. Optimum Life-Cycle Design of Orthotropic Steel Deck Bridges. Steel Structures, 2001.

ERDAL, F., DOGAN, SAKA, M. P. Optimum design of cellular beams using harmony search and particle swarm optimizers. Journal of Constructional Steel Research, v. 67, n. 2, p. 237-247, 2011.

FERRO K.B, ALVES, E.C. Developed interactive system to design of hollow core slabs. Procedures of 61° Brazilian Congress of Concrete. ISSN 2175-882, 2019. (In Portuguese)

FIOROTTI, K.M; CALENZANI, A.F.G., ALVES, E.C. Optimization of steel beams with external pretension, considering the environmental and financial impact. ASIAN JOURNAL OF CIVIL ENGINEERING. 2023.

GUIMARAES, S. A. ; KLEIN, D. ; CALENZANI, A. F. G. ; ALVES, E. C. . Optimum design of steel columns filled with concrete via genetic algorithm: environmental impact and cost analysis. REM - INTERNATIONAL ENGINEERING JOURNAL, v. 75, p. 117-128, 2022.

KAVEH A., ARDALANI S.H, (2016). Cost and CO2 Emission Optimization of Reinforced Concrete Frames Using ECBO Algorithm. ASIAN JOURNAL OF CIVIL ENGINEERING, 17(6), 831-858

KAVEH A., IZADIFARD R.A., MOTTAGHI L., (2020). Optimal Design of Planar RC Frames Considering CO2 Emissions Using ECBO, EVPS and PSO Metaheuristic Algorithms, JOURNAL OF BUILDING ENGINEERING, 28, 101014

KAVEH A, MOTTAGHI L, IZADIFARD RA,(2022). Optimization of columns and bent caps of RC bridges for cost and CO2 emission, Periodica Polytechnica Civil Engineering 66 (2), 553-563

KOCIECKI M., ADELI H. Shape optimization of free-form steel space-frame roof structures with complex geometries using evolutionary computing. Engineering Applications of Artificial Intelligence, 38, p. 168–182, 2015.

KRIPAKARAN P, HAL B, GRUPTA A. A genetic algorithm for design of moment-resisting steel frames. Structural and Multidisciplinary Optimization, 2011.

KRIPKA M, MEDEIROS G.F, LEMONGE A.C. Use of optimization for automatic grouping of beam cross-section dimensions in reinforced concrete building structures. Engineering Structures, v. 99, p. 311-318, 2015.

KUAN-CHEN-FU F.A, ZHAI Y, ZHOU S. Optimum Design of Welded Steel Plate Girder Bridges Using a Genetic Algorithm with Elitism. Journal of Bridge Engineering, 10 Edition, p. 291-301, 2005. Disponível em: https://doi.org/10.1061/(ASCE)1084-0702(2005)10:3(291)

LIPPIAT B. BEES. 4.0: Building for Environmental and Economic Sustainability Technical Manual and User Guide - NIST, 2007.

LEUÉVANOS-ROJAS A, LÓPES-CHAVARRÍA S. MEDINA-ELIZONDO M, KALASHINIKO, VV. Optimal design of reinforced concrete beams for rectangular sections with straight haunches, Revista de La Construccion, vol.19 no.1 pp. 90-102, 2020.

LOW, H. F., KONG, S.H., KONG, D., PAUL, S.C. Interface slip of post-tensioned concrete beams with stage construction: Experimental and FE study. Computers and Concrete, Vol. 24, No. 2 (2019) 173-183

MAGHSOUDI M., MAGHSOUDI A.A. (2019). Finite Element and Experimental Investigation on the Flexural Response of Pre-tensioned T-Girders. International Journal of Civil Engineering, vol. 17, 541-553.

MALVIEIRO J, RIBEIRO D , SOUSA C, CALÇADA, R. (2018), Model updating of a dynamic model of a composite steel-concrete railway viaduct based on experimental tests. Engineering Structures, v. 164, p. 40–52, 2018. Disponível em: < https://doi.org/10.1016/j.engstruct.2018.02.057.>

MOTLAGH H.R.E, RAHAI A. (2022) Prediction of Long-Term Prestress Loss in Prestressed Concrete

Beam with Corrugated Steel Web. International Journal of Civil Engineering, vol. 20, 1309-1325.

NETTO, P.M.; CALENZANI, A.F.G.; ALVES, E.C. (2023), "Optimum design of prestressed steel beams via genetic algorithm." *REM – Internationl Engineering Journal*. Ouro Preto. v.76.

PARK H.S, KWON B, SHIN Y, KIM Y, HONG T. CHOI SW. (2013), "Cost and CO2 emission optimization of steel reinforced concrete columns in high-rise buildings", Energies, 6(11), 5609–5624. <https://doi.org/10.3390/en6115609>.

PAYA-ZAFORTEZA I, YEPES V, HOSPITALER A, GONZÁLEZ-VIDOSA, F. (2009), "CO2-optimization of reinforced concrete frames by simulated annealing", Engineering Structures, 31(7), 1501–1508. https://doi.org/10.1016/j.engstruct.2009.02.034

PRENDES-GERO, M.B, BELLO-GARCÍA A, COZ-DÍAZ JJ, DOMÍNGUES F.J.S, NIETO P.J.G. Optimization of steel structures with one genetic algorithm according to three international building codes. Revista de La Construccion, April, 2018.

SANTORO J.F, KRIPKA M. Minimizing environmental impact from optimized sizing of reinforced concrete elements. Computers and Concrete, v. 25, n. 2, p. 111-118, 2020.

SENOUCI A.B, AL-ANSARI M.S. Cost optimization of composite beams using genetic algorithms. Advances in Engineering Software, v. 40, n. 11, p. 1112-1118, 2009.

SINAPI (2020). Sistema Nacional de Preços and Índices para a Construção Civil - Caixa Econômica Federal, Vitória, Espírito Santo, Brasil.

TORMEN A.F, PRAVIA Z.M.C; RAMIRES F.B, KRIPKA M.(2020), "Optimization of steel concrete composite beams considering cost and environmental impact". Steel and Composite Structures, 34(3), 409-421. <https://doi.org/10.12989/scs.2020.34.3.409>.

VAHIDI M, VAHDAN S, RAHIMIAN M, JAMSHIDI N, KANEE A.T. (2019), "Evolutionary-base finite element model updating and damage detection using modal testing results". *Structural Engineering and Mechanics.* v. 70, n. 3, p. 339-350. https://doi.org/10.12989/sem.2019.70.3.339

CHENG, X., HONG, J., MAN, L., LI, G. Flexural performance test of a prestressed concrete beam with plastic bellows. Structural Engineering and Mechanics, vol. 79, No. 2 (2021) 223-235

YEPES V., MARTÍ J.V, GARCÍA-SEGURA T. (2015) Cost and CO2 emission optimization of precast–prestressed concrete U-beam road bridges by a hybrid glowworm swarm algorithm. Automation in Construction, v. 49, p. 123-134, 2015.

YILDIRIM H.A, AKCAY C. Time-cost optimization model proposal for construction projects with genetic algorithm and fuzzy logic approach, Revista de La Construccion, vol.18 no.3 pp. 554-567, 2019.